

Effect of Cocrystallization on Kinetic Parameters of High-Density Polyethylene/Linear Low-Density Polyethylene Blend

S. K. RANA

Department of Textile Technology, Indian Institute of Technology, New Delhi 110 016, India

SYNOPSIS

The isothermal crystallization kinetics of a binary melt blend of high-density polyethylene (HDPE)/linear low-density polyethylene (LLDPE) is presented. An effort was made to understand the phenomenon of cocrystallization between these two constituting components of the blend with the help of kinetic parameters. The analysis based on the Avrami exponent entails that both HDPE and LLDPE undergo individual seeding of nuclei and they merge with each other in the growth process to form cocrystallites. The incorporation of the LLDPE segment in the HDPE crystallites progressively dilutes the properties of HDPE in the blend. The half-time of crystallization ($t_{1/2}$) shows variation in three distinct stages: The $t_{1/2}$ increases slowly in the region of 0–30% LLDPE content (HDPE-rich blend), remains constant in the 30–70% LLDPE-containing region (middle region of blend composition), and increases sharply thereafter. These variations of $t_{1/2}$ quite appreciably explain the change in % crystallinity, the Avrami exponent, and crystallite-size distribution. These observations were further supported by the small-angle light-scattering experiment. © 1996 John Wiley & Sons, Inc.

INTRODUCTION

The nucleation rate, growth rate, and morphology¹ help in understanding the entire crystallization process. The necessity of studying crystallization kinetics lies with the fact that the properties of a polymer are generally governed by the content and habits of crystallites (i.e., morphology). The differential thermal traces of phase transformation from the amorphous phase to the crystalline phase provides sufficient data to characterize the crystallization process. The crystallization, when it proceeds isothermally, is mostly treated quantitatively with the help of the Avrami theory,² which has subsequently been simplified by Evans,³ Morgan,⁴ and Mandelkern⁵ for the trailing part of the crystallization. The expression correlates the elapse time (t), the crystallization time-dependent crystallinity (X_t), and the maximum achievable crystallinity (X_E) with the Avrami exponent (n) and the rate constant (K) as

$$X_t = X_E \{1 - \exp(-kt^n)\} \quad (1)$$

Equation (1) may be rearranged to the well-known form:

$$\log\{-\ln(1 - X_t/X_E)\} = \log(k) + n \log(t) \quad (2)$$

The plot of $\log\{-\ln(1 - X_t/X_E)\}$ against $\log(t)$ would provide a straight line with slope n and intercept $\log(k)$.

This article discusses the effect of cocrystallization^{6,7} on crystallization parameters, viz., half-time ($t_{1/2}$), rate (k), and the Avrami exponent (n) of crystallization of HDPE/LLDPE blend.

EXPERIMENTAL

Materials

The high-density polyethylene (HDPE) (Hostalene GF 7745 F) used for this study was a product of Polyolefin Industries Ltd., Bombay, India. The linear low-density polyethylene (LLDPE) (Dowlex

2740 E), an octene-based copolymer, was a product of Dow Chemicals, USA. The properties of these two pure polymers are listed in Table I.

Blend Preparation

The solid chips of HDPE and LLDPE were mixed in a tumble mixer so as to form a uniform composition all through the batch size. This uniformly mixed feed was then melt-blended in a single-screw extruder (Betol 1820) with an L/D ratio of 17 and a screw speed of 22 rpm. The temperature profile of the extruder was kept as 160, 200, and 210°C at the feed zone, compression zone, and metering zone, respectively. The die-end was kept at 200°C. The extruded strands were cooled in water maintained at 30°C and subsequently granulated after allowing a maturation time of 8 h.

Compression Molding

The compression molding was done at $(165 \pm 2)^\circ\text{C}$ at a pressure of 300 kg/cm² for 2 min followed by solidification under nominal pressure for another 2 min. The films so-obtained were quenched in water at 30°C. These films were used for both differential scanning calorimetric (DSC) analysis and small-angle light-scattering experiments.

Measurements

Differential Scanning Calorimeter

The powdered sample weighing about 10 mg was taken in an aluminum crucible and crimped for the DSC experiment on a Perkin-Elmer DSC 7 thermal system. The samples were heated to 165°C and kept for 2 min under a nitrogen blanket. The molten mass was then rapidly cooled to 115°C and held isothermally at this temperature to obtain a crystallization exotherm. The % crystallinity is calculated as

$$\text{Crystallinity } (X_c, \%) = [\Delta H / \Delta H_c] \times 100$$

where ΔH is the heat of crystallization of the sample, and ΔH_c , the heat of crystallization of 100% crystalline polyethylene.

Small-angle Light-Scattering Experiment

The H_v light-scattering instrument and thin compression-molded films were used for this experiment. The " H_v " designates the direction of the polarizer and analyzer with one in the horizontal and the other in the vertical position, respectively.

Table I Characteristic Properties of HDPE and LLDPE

Properties	HDPE	LLDPE
$[\eta]$ at 111°C in decalin (dL/g)	1.10	1.50
T_m (°C)	131	126
Melt flow index (g/10 min)	0.75	1.00
Density (g/cc)	0.952	0.952
Tensile at yield (MPa)	24.5	19.3
CH ₃ /100 Carbon	1.81	3.00
X_c %	46	36

RESULTS AND DISCUSSION

Differential Scanning Calorimetry

Figure 1 represents isothermal crystallization exotherms (ICE) of HDPE, LLDPE, along with some of their selected blends. The necessary characteristic data of these ICE are presented in Table II. On close examination, Figure 1 reveals that the exothermic peak of HDPE is narrower in width and has a greater area in comparison to that of LLDPE. The ICE of blends resemble mostly the ICE of the major constituent; however, the exothermic peak of 50/50 blend matches to that of HDPE in peak area and LLDPE in peak width.

The crystallization behavior of the HDPE/LLDPE blend was reported earlier⁶ and it was shown that the singlet crystallization exotherm characterizes cocrystallinity between HDPE and LLDPE. The phenomenon of cocrystallization between these two components had further been supported by an X-ray diffraction pattern of these blends. With the same analogy, the singlet peak nature of all the ICE may also be attributed as the criteria of cocrystallization.

Figure 2 shows the variation of the degree of crystallinity with time as the molten mass is allowed to crystallize isothermally (i.e., at 115°C). Qualitatively, all these curves are similar; however, they differ considerably on quantification. HDPE shows the highest crystallinity among all the samples with a magnitude of 61%, while LLDPE achieved the crystallinity of around 39% after the completion of the isothermal run. The smooth transformation of the crystallinity value from HDPE to LLDPE is apparent as the % LLDPE content in the blend increases.

The Avrami Plot

The plot of $\log\{-\ln(1 - X_t/X_E)\}$ vs. $\log(t)$, as per eq. (2), is shown in Figure 3. Some points deviate

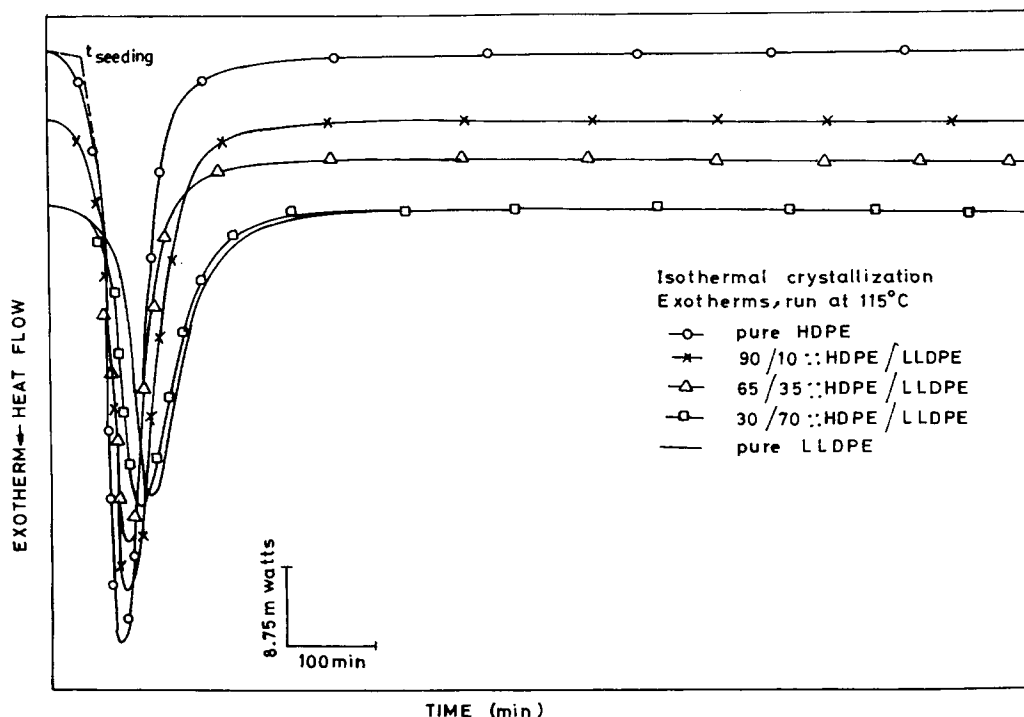


Figure 1 Isothermal crystallization exotherms of HDPE, LLDPE, and some selective blends.

from the straight-line behavior both at the beginning and at the end of crystallization. At the beginning, it requires adequate induction time to seed the crystallites; therefore, the rate is slow. Similarly, at the end, when crystallites impinge on each other, the rate of crystallization proceeds extremely slowly. Therefore, the straight line is drawn to represent the average behavior of the crystallization rate and the Avrami exponent (n) and the rate constant (k) are calculated from the slope of the curve and intercept, respectively. The half-time of crystallization ($t_{1/2}$) is calculated by applying the formula

$$t_{1/2} = (\ln 2/k)^{1/n} \quad (3)$$

The numerical value of these crystallization parameters (i.e., n , $t_{1/2}$, % crystallinity, etc.) are listed in Table II.

The $t_{1/2}$ (i.e., $(t_{1/2})_{ob}$) as seen from Figure 2 is also shown in Table II, which could be compared to the calculated values. The trends of variation of $(t_{1/2})_{ob}$ depicts a similar variation; however, the values differ considerably in these two cases. The higher $(t_{1/2})_{ob}$ to that of $t_{1/2}$ calculated values are due to the fact that the growth of crystallites greatly impaired at the trailing end of crystallization. The growing crystallites impinge on each other, and as a result, the rate of crystallization decreases significantly. The slow seeding of crystallites in the beginning of crystallization also contributes considerably to the de-

Table II Isothermal Crystallization Kinetic Parameters of HDPE/LLDPE Blend

Sample Wt % HDPE : LLDPE	Crystallinity (%)	n	$t_{1/2}$ (min)	$t_{(1/2)ob}$ (min)	$k \times 10^4 \text{ min}^{-1}$
100 : 0	60.5	3.09	10.88	40.0	4.34
90 : 10	57.8	2.75	15.34	45.0	3.80
75 : 25	54.8	2.39	19.03	52.2	6.06
65 : 35	51.3	2.60	21.33	—	10.21
50 : 50	51.2	2.30	15.75	50.5	12.21
30 : 70	46.3	2.22	24.21	52.2	13.05
20 : 80	44.0	2.12	29.29	54.5	13.06
0 : 100	37.8	2.05	50.57	57.6	2.23

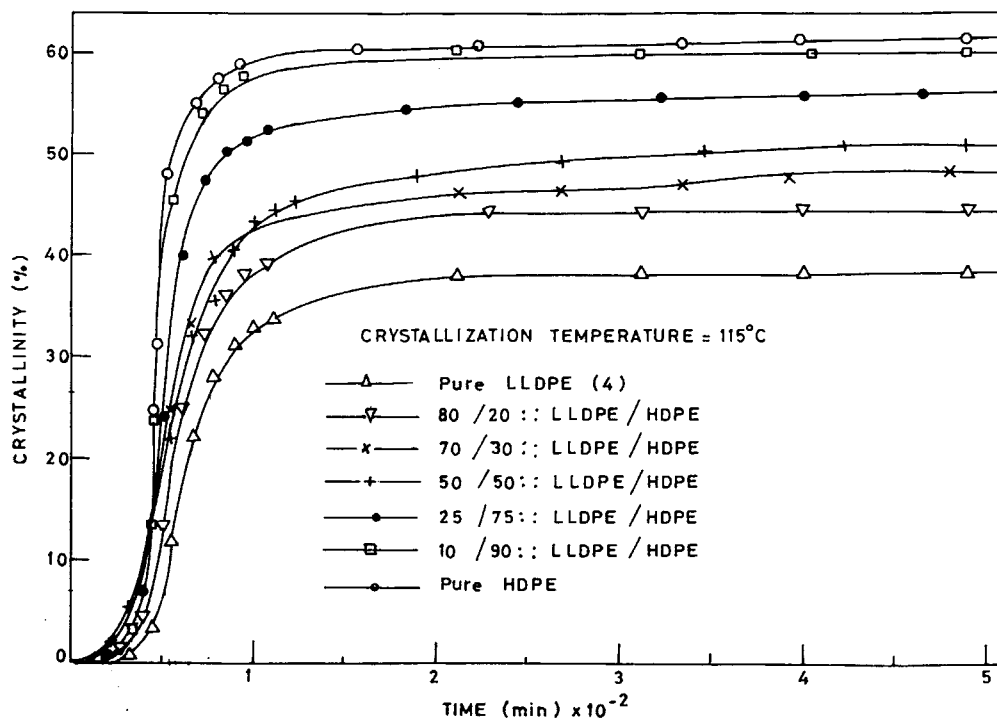


Figure 2 Variation of % crystallinity with respect to time of crystallization of HDPE/LLDPE blend.

viation of $t_{1/2}$ calculated from eq. (3) to the $(t_{1/2})_{ob}$ values observed.

Figure 4 shows the variation of % crystallinity, n , and $t_{1/2}$ against blend composition. The % crystallinity curve depicts a slight nonlinear decrease with increase in % LLDPE content in the blend. The % crystallinity maintains almost a constant value up to 10% LLDPE content at 61% crystallinity. A rapid decrease in crystallinity from 61 to 51% is seen at around 30% LLDPE content (Fig. 4). The crystallinity value remains constant at the 51% level in the 30–70% range of LLDPE content. The decrease in the % crystallinity is also apparent in the 70–100% LLDPE-containing region. A point to note is that the crystallinity reported in Table I is the nonisothermal crystallinity, scanned at the rate of 10°C/min, of the as-obtained samples, which is considerably lower to that of the isothermal crystallinity and this primarily seems to be due to the difference in test conditions.

The $t_{1/2}$ varies nonlinearly with blend composition (Fig. 4) and the trends of variation of $t_{1/2}$ may well be divided into three regions: (i) In the HDPE-rich region (i.e., 0–30% LLDPE-containing blend), $t_{1/2}$ increases more sharply with increase in the LLDPE content than does (ii) the middle region of the blend composition (i.e., 30–70% LLDPE-containing blend), and (iii) in the LLDPE-rich (i.e., 70–100% LLDPE-containing blend) blend, $t_{1/2}$ rises steeply

in value with increase in % LLDPE content. However, a linear decrease in the Avrami exponent n is observed with increase in the % LLDPE content from a value of 3.09 for HDPE to 2.0 for LLDPE (Fig. 4) with little deviation of few data points. These Avrami exponents are slightly higher than are the nonisothermal crystallization data reported earlier,⁶ which were 2.94 and 1.72, respectively, for HDPE and LLDPE. This slightly higher values of n for isothermal crystallization seems to be due to the conducive thermal environment provided for the growth of crystallites.

The decrease of % crystallinity in the HDPE-rich region may be attributed to the obstruction in mobility of HDPE chain segments by the LLDPE chains, which decreases the rate of crystallization—hence, the % crystallinity. However, in the range of 0–10% LLDPE, where the crystallinity almost remains constant, the hindrance on chain mobility caused by the LLDPE was perhaps balanced by the increase in free volume due to the presence of bulky octene groups in the LLDPE chains. In the middle range of the blend composition, both the constituents actively take part in crystallization and their relative concentration is not instrumental in playing a significant role. The % crystallinity in this region is quite nearer to the average value. In the LLDPE-rich blend, the addition of more labile HDPE chains, as it has fewer pendant groups and no bulky com-

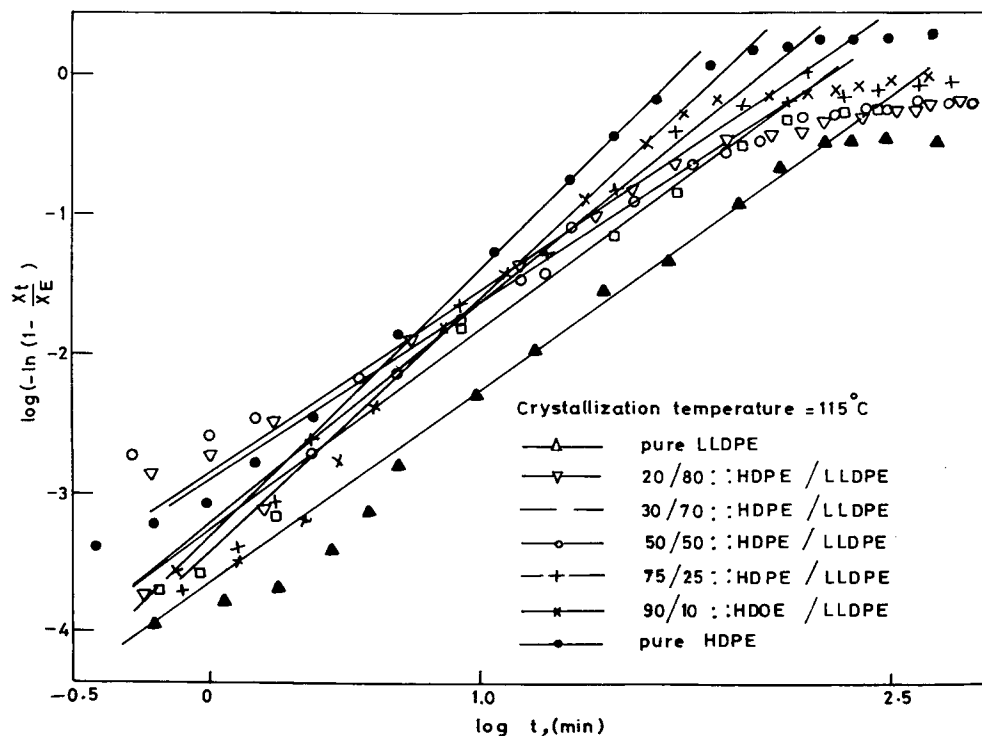


Figure 3 Avrami plots of crystallization parameters of HDPE/LLDPE blend.

moner, helps in increasing the % crystallinity as the % LLDPE decreases in the blend.

The $t_{1/2}$ represents the overall behavior of the crystallization kinetics. The lower the value of $t_{1/2}$, the faster would be the rate of crystallization, which also indicates the smaller crystallite sizes and narrower crystallite size distribution. On the other hand, a polymer with a high $t_{1/2}$ value would provide a material with big crystallites, wide crystallite size distribution, and low % crystallinity. The lowest $t_{1/2}$ value in the HDPE-rich blend, as discernible from Figure 4, may be responsible for lowest crystallite size,⁶ narrowest crystallite size distribution (i.e., narrow peak width of crystallization exotherm; see Fig. 1), and the highest % crystallinity. The nearly constant $t_{1/2}$ over a 30–70% range of LLDPE-containing blends seems to tailor the plateau type of crystallinity when compared with blend composition, while the gradually steep rise of $t_{1/2}$ with increasing LLDPE content (Fig. 2), owing to the slow seeding and growth of crystallites, could be actively interfering in decreasing the % crystallinity systematically with increase in LLDPE content. However, the discrepancy in the trends of variation of % crystallinity reported earlier⁶ were due mainly to the variation of the crystallizing condition. The data reported earlier were of injection-molded samples which were quite thick and underwent unaided crystallization to the

room temperature from the sample freezing temperature. The samples studied for characterization by isothermal crystallization are compression-molded and isothermally crystallized.

The Avrami exponents shown in Table II have mostly fractional values. The significance of the fractional values of the Avrami exponent is difficult to appreciate at the present understanding. The integral values up to 4 are attributed to different types of seeding and growth of crystallinity^{8–12} for linear polyethylene. Therefore, they could either be considered as representing the nearest integral value or an average contribution of more than one type of seeding of crystallites simultaneously occurring and their growth each conforming to different integral value of the Avrami exponent n . The integral values close to the fractional values may help in better perception of the crystallization process for pure components in the purview of widely accepted conventions.¹² Since both the components undergo cocrystallization⁶ in the present system (i.e., HDPE/LLDPE blend), it is reasonable to expect the constituting components to have identical growing crystallites which would allow the cocrystallization to take place. The smallest value of the Avrami exponent n obtained in the total range of blend composition for HDPE/LLDPE blend is 2. This value of n entails the sheaflike or distorted spherulitelike growing crystallites.^{12,13} Furthermore, considering a

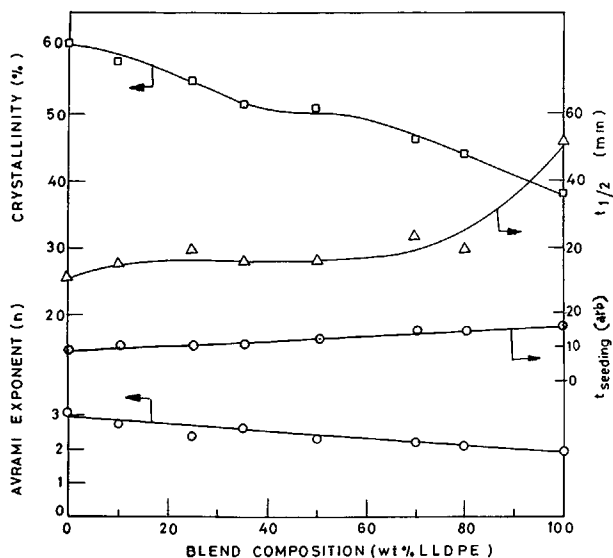


Figure 4 Plot of % crystallinity, $t_{1/2}$, Avrami exponent, and $t_{seeding}$ as a function of blend composition.

similar sequence of monomer in these polymers (i.e., ethylene unit) except some discontinuities due to the presence of the comonomer in the LLDPE, one would expect similar types of crystallites for both HDPE and LLDPE. Thus, the difference in n may be visualized as due to the variation in the types of seeding of nucleus. The HDPE with higher Avrami value may have sporadic seeding (i.e., Avrami exponent in excess of 2 which is equal to 1 could be attributed to this type of seeding), whereas LLDPE with a lower Avrami value seems to have instantaneous seeding of the nucleus (which accounts for this part of Avrami exponent to be equal to 0). The systematic decrease of n values with the increase in LLDPE content in the blend may be assumed due to the gradual decrease of sporadic to instantaneous seeding. The inflexion of curve in the ICE (shown as dotted line in Fig. 1) in the left-hand side represents the seeding time ($t_{seeding}$) of the nucleus. From Figure 1, it is discernible that the seeding time of HDPE is the least and that of LLDPE the highest. The blends maintain intermediate values. This seeding time plot against blend composition (Fig. 4) shows a linear variation which reinforces the belief of systematic linear variation of the type of seeding of the nucleus with the change in LLDPE content.

Small-angle Light Scattering

The H_v scattering patterns of HDPE, LLDPE, and the 50/50 blend are shown in Figure 5. The scattering pattern suggests a sheaflike^{12,13} and/or distorted spherulite-type crystalline growth for all three sam-

ples. The rest of the blend samples show a similar scattering pattern (not shown in Fig. 5).

In essence of the discussion of the Avrami exponent and the light-scattering experiment which indicate different types of seeding and similar growing crystallites (i.e., sheaflike for both the cases), one would expect the combination of these different types of nuclei of two constituting polymers to form

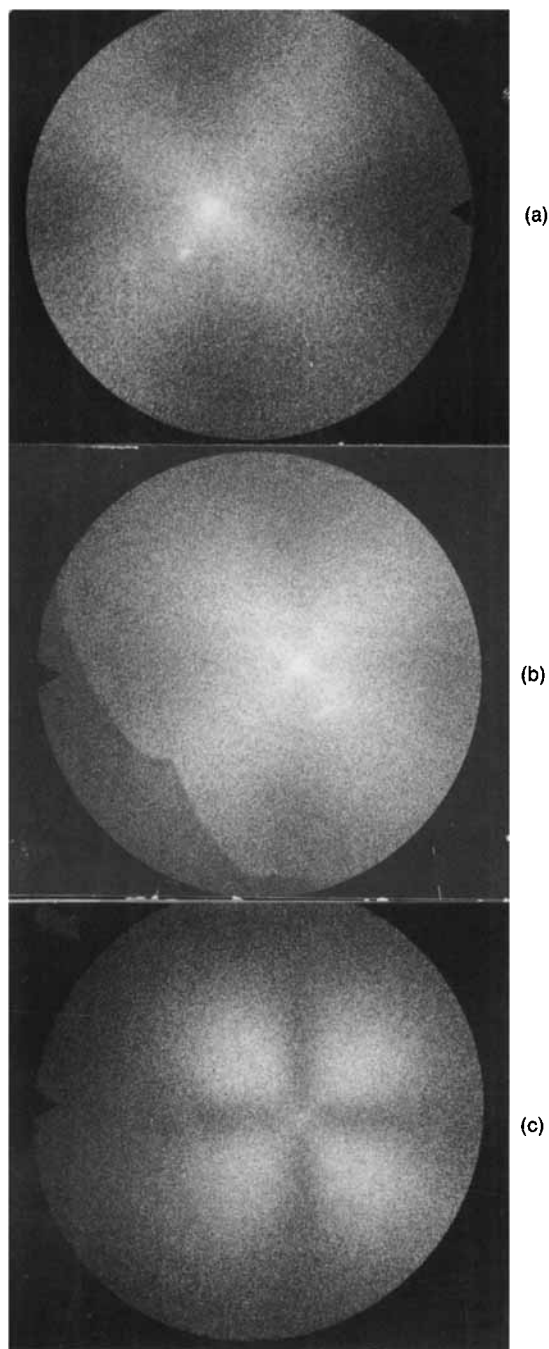


Figure 5 (a-c) Small-angle light-scattering pattern of (a) HDPE, (b) 50/50 blend, and (c) LLDPE.

cocrystallites (i.e., mixed crystallite) in the process of crystallite growth. Although the structural organization of these crystallites are similar, the property of the blend depends on the presence of comonomer units near the crystalline boundary which may impart some sort of destabilizing force onto the crystallites. The increase in the LLDPE content in the blend contributed to the systematic decrease of the melting temperature of the blend as reported earlier.⁶

Therefore, the linear variation of the Avrami exponent with blend composition (Fig. 4) may thus be assumed to comprise two parts:

- (i) The blend composition invariant part and
- (ii) The blend composition variant part.

The blend composition invariant part of the Avrami exponent is equal to 2, which indicates the sheaflike and/or distorted spherulite-type growing crystallites for HDPE, LLDPE, and their blends, whereas the blend composition variant part of the Avrami exponent, ranging from 1 to 0, corresponds to the sporadic seeding that arises from HDPE and an instantaneous type of seeding of the nucleus from LLDPE, respectively. The blends possess a combination of both types of seeding of crystallites and contributed to the fractional values of the Avrami exponent.

CONCLUSION

The HDPE and LLDPE blend manifests a singlet crystallization exotherm, which is ascribed to the cocrystallization between these constituting components. The similarities in their chemical structure may be accountable for their affinity toward cocrystallization. The blending of HDPE with LLDPE shows a pronounced effect on the parameters of the crystallization kinetics, viz., % crystallinity, $t_{1/2}$, and the Avrami exponent.

The % crystallinity shows variation on three zones due to the addition of LLDPE in HDPE. The addition of LLDPE in the HDPE-rich blend (i.e., 0–30% LLDPE content) shows a marginal effect on the % crystallinity up to 10% LLDPE content. Thereafter, a gradual decrease in the % crystallinity

with the increase in LLDPE content is registered (Fig. 4). In the middle range of blend composition (i.e., 30–70% LLDPE content), the % crystallinity remains almost constant, while in the LLDPE-rich blend (i.e., 70–100% LLDPE content), the % crystallinity decreases systematically toward the % crystallinity value of pure LLDPE.

Similar but opposite trends of the variation of $t_{1/2}$ to that of % crystallinity is observed (Fig. 4). The variation % crystallinity may better be described with the help of trends in the variation of $t_{1/2}$. The small magnitude of $t_{1/2}$ signifies the rapidly crystallizing mass and, hence, for similar crystallization, peak broadening would provide a higher % crystallinity with less variation in the distribution of the crystallite sizes.

Individual seeding of nuclei and the mixed growth of the crystallites are inferred from the analysis based on the Avrami exponent of the blend. The formation of cocrystallites thus may result from the merging of these individual crystallites in the growth process of the crystallization.

REFERENCES

1. A. Sharples, Editor, *Introduction to Polymer Crystallization*, Edward Arnold, London, 1975.
2. M. Avrami, *J. Chem. Phys.*, **7**, 1103 (1939); **8**, 212 (1940); **9**, 177 (1941).
3. F. V. Evans, *Trans. Faraday Soc.*, **41**, 365 (1945).
4. L. B. Morgan, *Philos. Trans. Soc. A*, **248**, 13 (1954).
5. L. Mandelkern, *Chem. Rev.*, **56**, 930 (1956).
6. A. K. Gupta, S. K. Rana, and B. L. Deopura, *J. Appl. Polym. Sci.*, **44**, 719 (1992); **46**, 99 (1992); **49**, 477 (1993); **51**, 231 (1994).
7. S. K. Rana, PhD Thesis, IIT Delhi, India.
8. A. Jezorney, *Polymer*, **19**, 1142 (1948).
9. J. N. Hay and Z. J. Perzekop, *J. Polym. Sci. Polym. Phys. Ed.*, **16**, 81 (1978).
10. J. N. Hay and P. J. Mills, *Polymer*, **23**, 1380 (1982).
11. J. Rabesiaka and A. J. Kovacs, *J. Appl. Phys.*, **32**, 2341 (1961).
12. T. Hashimoto, Y. Murakami, N. Hayashi, and K. Kawai, *Polym. J.*, **6**, 132 (1974).
13. W. Chu and R. S. Stein, *J. Polym. Sci. A-2*, **8**, 489 (1970).

Received October 3, 1995

Accepted February 27, 1996